Desalination and Water Treatment
www.deswater.com

doi: 10.5004/dwt.2022.28605

265 (2022) 134–145
July

Raw clay for ibuprofen and chlortetracycline removal from aqueous solution

Kheira Addouch[a], Soumia Seddari[b], Hakima Cherifi[a,*], Radhia Yous[a], Razika Khalladi[b]

[a]*Laboratoire des Biomatériaux et des Phénomènes de Transferts LBMPT, Université de Médéa, Médéa 26000, Algérie, emails : ha_cherifi@yahoo.fr (H. Cherifi), kheiraaddouch@gmail.com (K. Addouch), radia_yr@yahoo.fr (R. Yous)*
[b]*Laboratoire des Matériaux et Environnement LME, Université de Médéa, Médéa 26000, Algérie, email: Soumiaseddari@yahoo.fr (S. Seddari), r_khalladi@yahoo.fr (R. Khalladi)*

Received 1 December 2021; Accepted 27 May 2022

ABSTRACT

This study aimed to evaluate the adsorption performances of local raw clay for the removal of ibuprofen (IBP) and chlortetracycline (CTC) well detected in aquatic environments. The CTC and IBP adsorption was carried out in batch system at different conditions. The results revealed the efficiency of this adsorbent without any modification at a concentration of 2 g/L, 293°K, and an initial concentration of pollutant 50 mg/L. The maximum adsorbed quantities of CTC and IBP are 24.515 and 14.005 mg/g at 120 and 90 min respectively. The effect of pH was almost negligible for both drugs. The raw clay samples before and after adsorption were analyzed by scanning electron microscopy coupled with energy-dispersive X-ray analysis and infrared spectroscopy. The results showed that the two pollutants were differently adsorbed on the tested clay. Kinetic study showed that the pseudo-second-order model fitted well the experimental data for both drugs, and the sorption results were best represented by Langmuir model ($0.04 < R_L < 0.7$ and $R^2 > 0.97$). The maximum Langmuir adsorption capacity at 293°K, is 47.65 for IBP and 64.65 mg/g for CTC. The sorption of both pollutants is exothermic. For the CTC spontaneous favorable physisorption was observed. However, Elovich model confirmed the chemisorption of IBP.

Keywords: Adsorption; Chlortetracycline; Ibuprofen; Isotherm; Kinetics; Raw clay

1. Introduction

Pollution of surface and ground water by pharmaceutical products is a serious environmental problem [1,2]. Pharmaceuticals known as emerging pollutants are a group of pollutant that are not controlled in the environment. They caused dangerous effects on all ecosystems [3]. These molecules reach aquatic bodies, through human secretion by leaching from land and water drainage or from industrial solid and liquid effluents [4].

Pharmaceutical residues were detected in aquatic environments in 1960, since that year, researchers have been interested in the related consequences related to the existence of these micro pollutants in the environment [5,6]. The main sources of these molecules are wastewater treatment plants (WWTP), health care establishments and the pharmaceutical industry [7].

Generally, the elimination of pharmaceutical pollutants is carried out at the level of wastewater treatment plants, their efficiency varies from 0% to 90%, and it depends on the properties of the substance to be eliminated [8,9]. Conventional methods do not eliminate this compounds, because their concentrations are very low (ng/L and μg/L) compared to other pollutants (pesticides, heavy metals, dyes, hydrocarbons), although they present a high biological activity. This situation is intensified progressively by the very great diversity of the drugs used and rejected mainly by urinary and fecal tract [8,10].

Among different pharmaceuticals often detected in water resources, we have anti-inflammatory drugs like

* Corresponding author.

1944-3994/1944-3986 © 2022 Desalination Publications. All rights reserved.

ibuprofen (IBP) and antibiotics like chlortetracycline (CTC) [5,11]. IBP is widely used as an analgesic, antipyretic as well as for the treatment of rheumatic disorders, it is low-soluble in water but it has a high mobility in aquatic environments [12,13]. It was reported that ibuprofen concentration in aqueous medium is usually high, because it is excreted in its initial form in the urine [14].

According to Lawrence et al. [15], ibuprofen decreases the number of Cyanobacteria in the biofilms exposed to this substance during development. Frequently, ibuprofen is degraded at wastewater treatment plants to its metabolites. Carboxy-IBP and hydroxy-IBP have been identified as the main first metabolites of IBP widely detected in effluents and environmental samples. These substances presenting ecological risk similar or higher to the original molecule [16], for this reason, many researchers are still interested on the elimination of this molecule [13,17].

Antibiotics are the most widely used pharmaceutical compounds around the world; they have received increasing attention as pollutants due to their hazardous and carcinogenic properties causing chronic poisoning to aquatic or terrestrial organisms. Indeed, antibiotics highly induced bacterial resistance in various environments [18,19]. Chlortetracycline is an antibiotic frequently used in human and veterinary medicine; it is one of the first Tetracycline invented in 1940. It contains four carboxylic rings and several ionizable functions [20,21]. The CTC is the most consumable drug in high concentrations in animal husbandry, it is excreted in its active form by the urinary and fecal tract, and consequently it affects soils and surface waters [22,23]. A study carried out by Puicharla et al. [24] showed that there is strong interaction between metal ions and CTC molecules in soil, which causes their accumulation in environment. Consequently, resistance to this antibiotic will increase leading to serious problems that threaten human and animal health. In addition, CTC can affect several microorganisms, aerobic and anaerobic, Gram positive and Gram negative [25].

At present, the effect of pollution by drug residues is still unknown because it is so difficult to detect them at low concentrations [8,15]. Several processes were used to eliminate pharmaceuticals from aquatic environments [26]. Adsorption was proved an easy method to be operated, cheap and efficient to remove organic and inorganic pollutants. Activated carbons are the most used adsorbents for their high adsorption capacity, however, preparation and regeneration techniques are very expensive, so researches investigated unconventional adsorbents with low cost such as: biomass, seaweeds, agricultural residues and clays [27].

Natural clays are aluminum silicates characterized by small particle size (2 μm), large specific surface, and charged surface, which facilitates interactions with pollutants. In addition, they are non-toxic, inexpensive and very abundant in nature [28,29]. Taking benefit of these properties, this work aimed to test natural clay for the sorption of CTC and IBP.

According to the literature, the elimination of ibuprofen and antibiotics by activated carbon [13,17,30,31], and by modified clays [20,32,33] are widely studied. In this work, the raw clay was used without any physical or chemical treatment that amplifies the cost or the inherence of the residue after remediation. The objective of this study is to investigate the adsorption efficiency of raw local clay, very abundant in Algeria, for the elimination of two drugs widely detected in aqueous effluents, namely ibuprofen and chlortetracycline. The experimental operating conditions such as the contact time, the initial pH, the concentration of the adsorbent, the initial concentration of the pollutant and the temperature were optimized in a single batch system. Kinetic and thermodynamic studies were carried out to examine the sorption nature and its relation with the efficiency of the clay to eliminate CTC and IBP.

2. Materials and methods

2.1. Materials

IBP (Fig. 1a) and CTC (Fig. 1b), were supplied by Saidal (Antibiotical Group of Médéa). Ethanol (C_2H_5OH), sodium hydroxide (NaOH) and hydrochloric acid (HCl) (95% purity), were provided by Sigma-Aldrich. The clay used in this work is obtained from Maghnia (North West of Algeria).

2.2. Methods

2.2.1. Adsorbent preparation

A mass of clay was dispersed in a volume of distilled water under stirring. After 8 h of stirring the mixture is allowed to settle. The supernatant water was analyzed by spectrophotometer Genesys 10 UV-Visible. The clay was washed several times, until that the optical density of the supernatant will be almost constant. After that, clay sample was dried at 40°C for 72 h, then crushed using a mortar and sieved. Particles smaller than 45 μm were retained for adsorption tests.

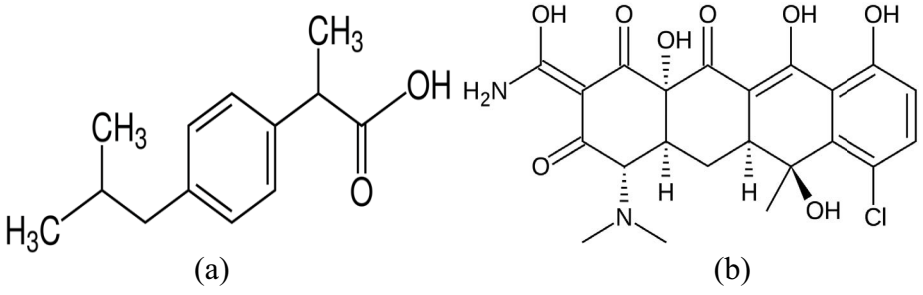


Fig. 1. Molecular structure of IBP (a) and CTC (b).

2.2.2. Adsorption essays

A stock solution (1 g/L) of IBP was prepared in alkaline medium using NaOH because IBP dissolves hardly and slowly in distilled water [34]. However, the CTC stock solution (1 g/L) was prepared in the presence of ethanol. All the experiments were realized by diluting the stock solution until the desired concentrations.

The adsorption tests were carried out in 250 mL Erlenmeyer's flask. The clay mass was brought into contact with 50 mL of pollutant solution. The mixture was stirred by a Heidolph Unimax 1010 shaker with at speed of 250 rpm. Samples were taken at: 5, 10, 20, 30, 60, 90, 120, 150, 180 min, and filtered using vacuum pump (0.45 μm) porosity after different contact time: The concentrations of IBP and CTC were determined by spectrophotometer Genesis10 UV-Visible at 222 nm (Fig. S1) and 370 nm (Fig. S2), respectively.

2.2.3. Kinetic study

Sorption kinetic was carried out at ambient temperature, and a fixed mass of adsorbent (0.1 g). First, the adsorbed mass per gram of adsorbent (Q_t) was calculated using Eq. (1). Then, the equilibrium time was determined from the curve Q_t vs. time (t), it corresponds to the moment when the pollutant concentration in the liquid phase remains constant. The maximum adsorbed quantity at equilibrium (Q_e) and the adsorption efficiency (E%) were calculated by Eqs. (2) and (3), respectively.

Moreover, the effect of various factors such as pH (pH = 3–10), initial concentration of pollutant (C_0 = 5–150 mg/L), concentration of adsorbent (C_a = 2–14 g/L) and temperature (T = 293–323°K) were investigated at equilibrium time. Optimal conditions were deduced from this parametric study. The pH was measured by HANNA pH meter. It is adjusted by the addition of NaOH (0.1 M) and HCl (0.1 M).

$$Q_t = \frac{\left(C_0 - C_t\right)V}{m} \tag{1}$$

$$Q_e = \frac{\left(C_i - C_e\right)V}{m} \tag{2}$$

$$\left(E\%\right) = \frac{\left(C_i - C_e\right)}{C_i} \times 100 \tag{3}$$

Three kinetic models were tested; the pseudo-first-order [35] the pseudo-second-order [36], and Elovich model [37], given by Eqs. (4)–(6), respectively:

$$\log\left(Q_e - Q_t\right) = \log Q_e - \frac{K_1}{2.303}t \tag{4}$$

$$\frac{t}{Q_t} = \frac{1}{k_2\left(Q_e\right)^2} + \frac{t}{Q_e} \tag{5}$$

$$Q_t = \frac{1}{B}\ln\left(AB\right) + \frac{1}{B}\ln t \tag{6}$$

2.2.4. Modeling of adsorption isotherms

The adsorption isotherms were studied using three models: Langmuir, Freundlich and Temkin (Table 1). Adsorption isotherms describe the quantity of pollutant adsorbed at equilibrium on the adsorbent (Q_e: mg/g) as a function of the residual concentration of the pollutant in the solution (C_e: mg/L). The adsorption isotherms of the two pollutants were carried out at optimal conditions.

2.2.5. Adsorbent characterization

A morphological and structural study of the adsorbent was carried out by scanning electron microscopy (SEM; FEI Quanta 650), and infrared spectroscopy Bruker Tensor II. The chemical composition was determined by quantitative energy-dispersive X-ray analysis (EDX) using Bruker EDS detector. All these analyses were performed for raw clay before and after adsorption. The pH of zero charge of the raw clay was determined by mixing 50 mg of clay with 50 mL of NaCl solution 0.01 M at different pH 2.0, 4.0, 6.0, 8.0, 9.0, and 10, then, the mixtures were stirred for 48 h. The difference between the final and the initial pH (ΔpH) was plotted against initial pH. The pH of zero charge is the pH at which the ΔpH equal zero [26].

3. Results and discussions

3.1. Kinetic study

Fig. 2 shows the variation of adsorbed quantity vs. time for IBP and CTC. The quantity of both drugs increases with the increase of time until equilibrium. For the IBP, the adsorption extent augments slowly to reach the maximum value of 14.005 mg/g after 120 min. There is no appreciable change between 120 and 180 min, implying attainment of equilibrium of the sorption. However, the CTC retention began from the first minutes of contact with the clay then remains almost constant with a maximum adsorbed quantity of 24.515 mg/g reached at 90 min. For both substances, the increase in the first stage of adsorption is due to the presence of a high number of free sites on the surface of the adsorbent. Nevertheless, the CTC molecules show a quick

Table 1
Isotherms equations

Isotherm model	Equation	Parameters	References
Langmuir	$Q_e = Q_m \frac{K_1 C_e}{1 + K_L C_e}$	Q_m (mg/g) K_L (L/mg)	[38]
Freundlich	$Q_e = K_f C_e^{1/n}$	N K_f (L/mg)	[39]
Temkin	$Q_e = B\ln A_T C_e$	A_T (L/mg) B (kJ/mol)	[40]

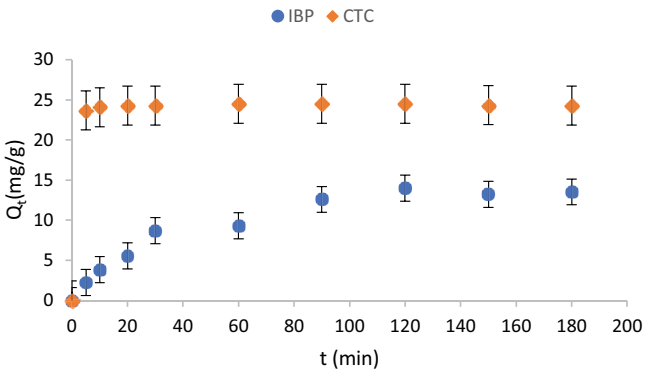


Fig. 2. Kinetic results of adsorption of IBP and CTC on raw clay (T = 293°K; C_a = 2 g/L; C_0 = 50 mg/L).

sorption rate and the equilibrium was reached quickly more than that of IBP. This behavior could be explained by the chemical structure of CTC (Fig. 1b). Where, the steric affinity of CTC probably improved its adsorption on the clay surface leading to a short equilibrium time. Indeed, CTC molecule shows divers chemical bounds (OH, NH_2, and ketone bounds) compared to the IBP. The equilibrium indicated the saturation of the active sites present on the solid surface and may be the presence of repulsion between the adsorbed molecules, and the non-adsorbed ones [3].

Table 2 represents the results of the kinetic study for both drugs. It reveals the poor fitting of the pseudo-first-order model to the experimental data (Fig. S3). On the other hand, the curves of the pseudo-second-order model (Fig. S4) show a good linear relation with a high R^2 (R^2 = 1 for the CTC and 0.97 for the IBP). In addition, the calculated adsorbed quantity (Q_{cal}) was very close to the experimental one (Q_{exp}). According to these results the adsorption process fits well the pseudo-second-order model. Moreover, the Elovich model (Fig. S5) fits well only the experimental data of IBP (R^2 = 0.96).

According to Metwally et al. [41] and El Bendary et al. [42], the pseudo-second-order model generally indicated that the process is chemisorption involving chemical bounds between the raw clay and the pollutants molecules. In addition, the Elovich model confirmed the chemisorption process in the case of IBP [43]. However, for the CTC the nature of the adsorption process could not be physical. Several studies have found that the adsorption of IBP on different adsorbents followed the pseudo-second-order model [12,28,34]. Also, the literature reported that the same result was obtained for the adsorption of CTC on raw clay [44].

3.2. Parametric study

3.2.1. pH effect

Fig. 3 represents the pH of zero charge (pH_{pzc}) of the adsorbent. It was found that pH_{pzc} = 7. The pH effect on the adsorption capacity of the two pollutants was carried out at a temperature of 293°K, with a clay concentration of 2 g/L and an initial concentration of 50 mg/L for each pollutant. The obtained results are shown in Fig. 4. At pH = 4, the ibuprofen is at a pH lower than its pKa (4.9). Clay has a negative charge (<pH_{pzc}) on its surface, which promotes interactions between the molecule and the adsorbent. On the other hand, in a basic medium, the pH is higher than the pH zero charge, the decrease in the adsorption capacity is remarkable, this is reflected by repulsion between the solute and the surface of the adsorbent [17]. The maximum removal rate of IBP is 56.02% at pH = 4. These results

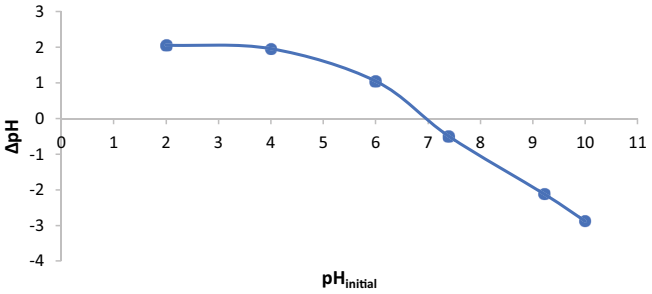


Fig. 3. Point of zero charge of raw clay.

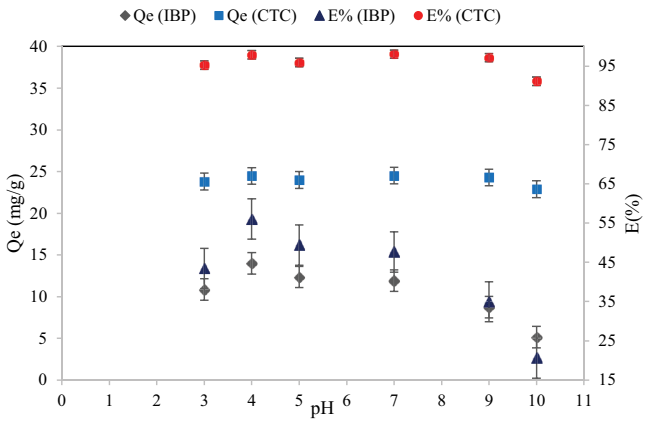


Fig. 4. Effect of pH on the adsorbed quantity and on removal rate of the two pollutants (C_a = 2 g/L; C_0 = 50 mg/L; T = 293°K).

Table 2
Pseudo-first-order and pseudo-second-order parameters for the removal of IBP and CTC onto raw clay

Molecules	Pseudo-first-order				Pseudo-second-order			Elovich		
	Q_{exp} (mg/g)	Q_{cal} (mg/g)	K_1 (min^{-1})	R^2	Q_{cal} (mg/g)	K_2 (g/mg min)	R^2	A (mg/g min)	B (g/mg)	R^2
IBP	14.005	11.904	0.0186	0.97	15.503	0.00263	0.97	0.62	0.964	0.964
CTC	24.515	13.533	00117	0.173	24.390	0.884	1	4.128	3.12	0.476

are in agreement with the results obtained by studies of Styszko et al. [27] and Khalaf et al. [34].

The influence of the pH on the adsorption capacity of CTC was determined under the same experimental conditions as the IBP, the results show a maximum capacity at neutral pH (pH = 7), and the removal efficiency varies from 91.15% to 98.06% in the interval pH = 3–10 (Fig. 4). Therefore, the pH has a non-obvious effect on the CTC sorption under these conditions. In general, adsorption efficiency may depend on the solution pH, especially when electrostatic interactions dominate the adsorption process [45].

3.2.2. Effect of adsorbent concentration and initial concentration of pollutants

The effect of the raw clay concentration was studied at 293°K and initial concentration of 50 mg/L for CTC and IBP. Fig. 5 shows that, the adsorbed quantity decreases significantly with the increase of the adsorbent concentration in the interval 2–14 g/L. This trend is typical for increasing the adsorbent dosage and it is ascribed to the agglomeration of clay particles. Hence, the number of accessible active sites is reduced and the diffusional path will be longer [42,46].

On the other hand, the effect of the initial concentration of the pollutant on the adsorption capacity of clay was studied at T = 293°K and 2.00 g/L of adsorbent. Fig. 6 shows that the retention capacity of clay increases with the increase of the initial concentration of the pollutant (CTC and IBP). Increasing the initial concentration of pollutant will augment the number of molecules in contact with the adsorbent surface. This behavior will increase the diffusion of the substances towards the support surface and consequently, this will overcomes the mass transfer resistance of the drugs between the aqueous and solid phases, then the adsorption capacity will increase [13,42,45]. According to Thiebault et al. [47], the maximum quantity of an anionic pollutant adsorbed on clay was observed for large solid–liquid ratios.

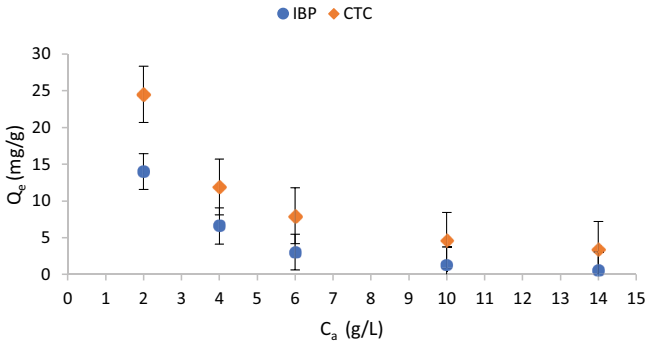


Fig. 5. Effect of the adsorbent concentration on the adsorbed quantity of CTC and IBP on raw clay (C_0 = 50 mg/L; T = 293°K).

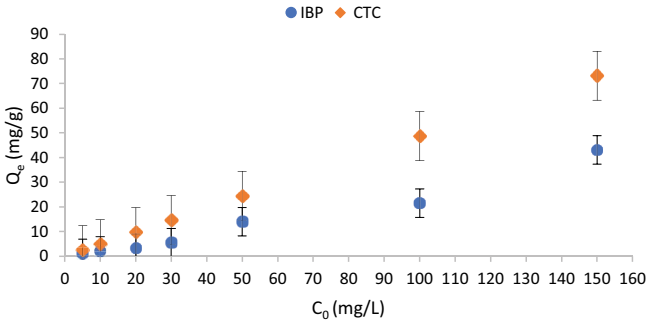


Fig. 6. Effect of initial concentration of CTC and IBP on the adsorbed quantity (C_a = 2 g/L; T = 293°K; pH = 7 for CTC; pH = 4 for IBP).

3.2.3. Effect of temperature

To demonstrate the influence of temperature on the adsorption process of CTC and IBP on clay, a series of experiments were carried out at different temperatures and under optimal conditions.

Fig. 7 shows a slight decrease in the adsorbed quantity of IBP in the range of 293–313°K as well as for the CTC. Therefore, it can be concluded that the temperature has a negligible influence on the elimination of the two pollutants in the interval of 293–323°K.

3.3. Modeling of adsorption isotherms

The results of isotherms modeling (Figs. S5–S7) are presented in Table 3.

Freundlich's model defines the adsorption mechanism on a heterogeneous surface [32]. Langmuir's model assumes that the adsorbent has a constant number of adsorption sites and each site is occupied by a single molecule [29,48]. In the case of the Langmuir isotherm (Table 3), the correlation coefficients are 0.97 and 0.98 for IBP and CTC respectively. The maximum adsorption capacity for CTC and IBP based on Langmuir model are 67.567 mg/g for CTC and 47.846 mg/g for IBP.

The dimension less equilibrium parameter of Langmuir R_L is defined by Eq. (7).

$$R_L = \frac{1}{\left(1 + K_L C_0\right)} \tag{7}$$

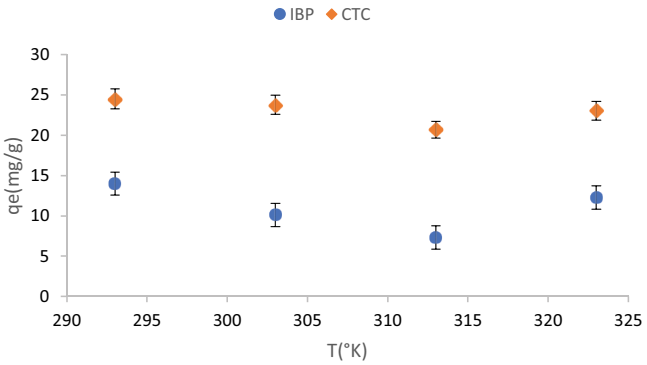


Fig. 7. Effect of temperature on the adsorbed quantity of CTC and IBP on raw clay (C_a = 2 g/L; C_0 = 50 mg/L; pH = 4 for IBP and 7 for CTC).

The value of R_L indicates the type of the isotherm to be either unfavorable (R_L > 1), linear (R_L = 1), favorable (0 < R_L < 1) or irreversible (R_L = 0) [49]. According to Table 3, the R_L values are between 0 < R_L < 1, 0.0473 and 0.714 for the CTC and IBP respectively, meaning that the adsorption of these drugs onto the studied clay is favorable. The smaller R_L value indicates a highly favorable adsorption. This result is consistent with Freundlich isotherm modeling where the adsorption of IBP and CTC was found favorable. Compared to Langmuir and Freundlich models, the Temkin modeling shows low correlation coefficients with both pharmaceuticals (R^2 < 0.840). Based on the correlation coefficients, Langmuir model represents better the adsorption of IBP and CTC on clay (R^2 = 0.97 and 0.98). These results are similar to those found in the literature [27,44].

3.4. Thermodynamic study

The thermodynamic parameters; enthalpy (ΔH), entropy (ΔS), and Gibbs free energy (ΔG) were calculated using Eqs. (8)–(10) [3,50].

$$\ln K_d = \frac{-\Delta H}{RT} + \frac{\Delta S}{R} \tag{8}$$

$$\Delta G = -RT \ln K_d \tag{9}$$

$$K_d = \frac{Q_e}{C_e} \tag{10}$$

The thermodynamic properties of adsorption are grouped in Table 4. In the case of CTC, ΔG was negative over the entire temperature range revealing the spontaneity of the adsorption process. Conversely, the IBP sorption is non spontaneous [46].

The enthalpy values obtained for IBP and CTC are –2.115 and –30.829 kJ/mol, respectively, indicating that this process is exothermic. The negative values of entropy indicate that the distribution of the molecules on the clay surface is important [43,48].

3.5. Characterization of adsorbents

The IR spectrum of the raw clay before adsorption (Fig. 8a) presents two bands in the range 3,200–3,800 cm^{-1}. The first band is located around 3,618.93 cm^{-1}, it is attributed to the vibrations of OH groups in the octahedral layer. And the second one (3,400.95 cm^{-1}) corresponds to the vibrations of the molecules of water adsorbed on the solid surface [28,37]. Another characteristic band is observed at 1,636.97 cm^{-1} corresponds to the deformation vibrations of adsorbed water molecules.

The most intense band located around 993.08 cm^{-1} is attributed to the elongation vibrations of the S–O bond. Bands appearing below 1,100 cm^{-1} are generally assigned to the vibration bands of the bonds: Si–O, Si–O–Si, Si–O–Al, Si–O–Mg [20,50].

The comparison of the spectrum of raw clay (a) with those after adsorption (Fig. 8b and c) shows a slight change after adsorption, where the intensity of some adsorption bands decreases. This reveals that the structure of the adsorbent was slightly altered during the adsorption of each pollutant.

The SEM image of the raw clay (Fig. 9a) shows the presence of many layers composed of aggregates of irregularly shaped particles. Fig. 9b and c show the swelling of clay particles after adsorption and also an agglomeration was observed. This behavior can be explained by the occupation of the free spaces and cavities by the adsorbed pollutant. The EDX analysis of the adsorbent reveals the presence of silicon (Si), carbon (C), oxygen (O) and aluminum (Al) as main elements as well as other elements such as: calcium (Ca), potassium (K), magnesium (Mg),

Table 3
Parameters of isotherm models obtained from the modelling results

	Langmuir				Freundlich			Temkin		
	Q_m (mg/g)	K_L (L/mg)	R^2	R_L	K_f (L/mg)	n	R^2	A_T (mg/g)	B_T (kJ/mol)	R^2
IBP	47.846	0.008	0.971	0.7142	0.574	0.887	0.929	0.196	10.995	0.688
CTC	67.567	0.402	0.980	0.0473	3.779	2.329	0.994	5.333	19.632	0.840

Table 4
Thermodynamic parameters of the adsorption IBP and CTC onto raw clay

Molecules	Temperature (K)	Q_e (mg/g)	ΔG (kJ/mol)	ΔH (kJ/mol)	ΔS (J/mol K)
IBP	293	14.005	+1.099	–2.115	–13.086
	303	10.113	+2.807		
	323	12.296	+1.946		
CTC	293	24.623	–8.511	–30.829	–78.750
	303	23.789	–5.753		
	323	23.040	–4.755		

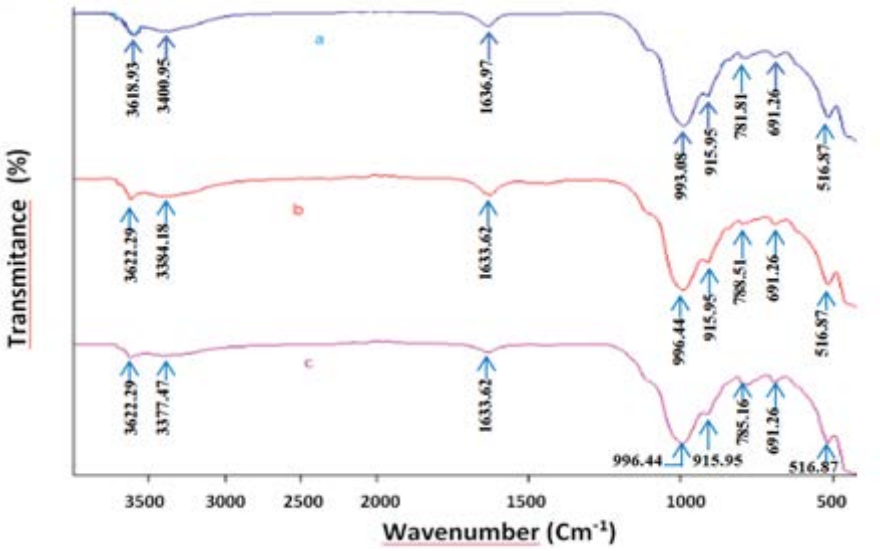


Fig. 8. Infrared spectrum of raw clay before sorption (a), after sorption of IBP (b) and after sorption of CTC (c).

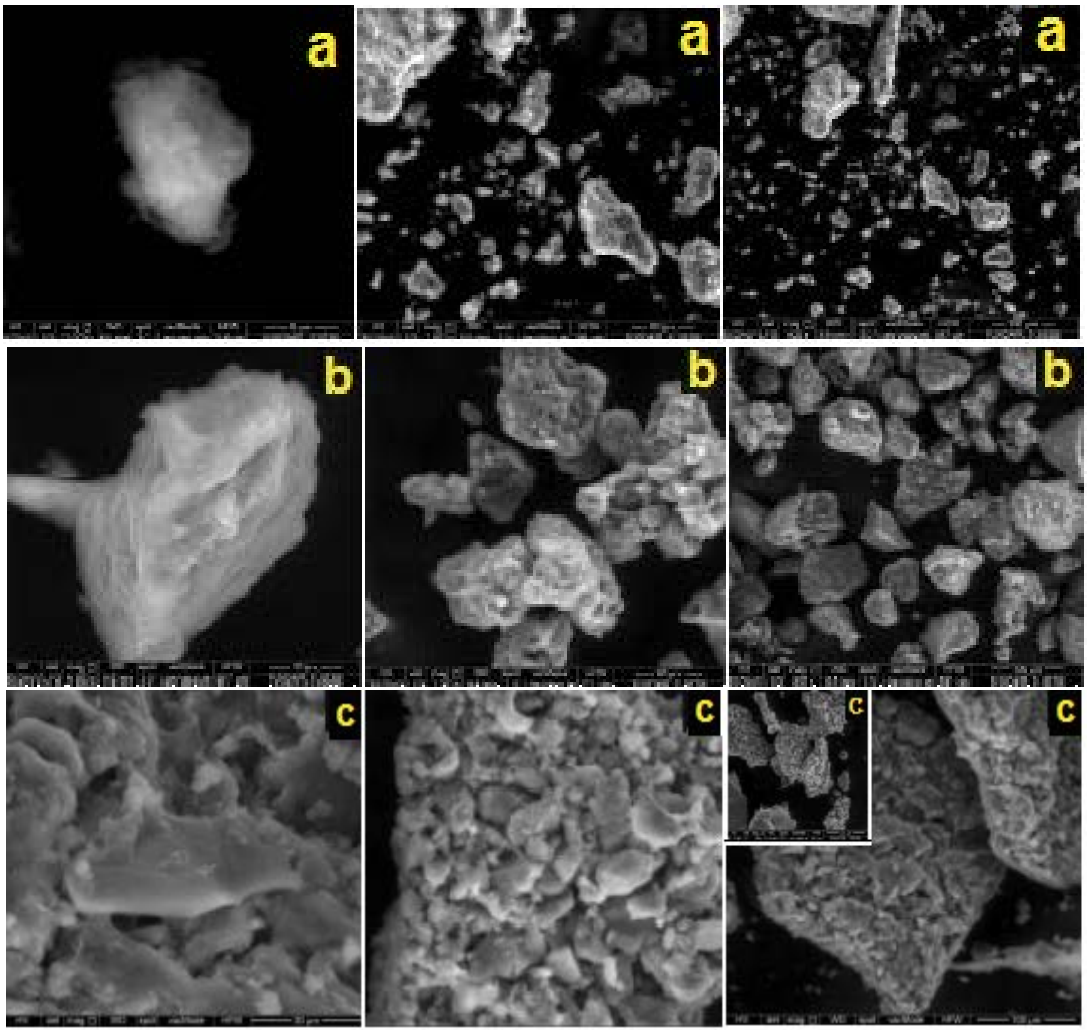


Fig. 9. SEM images of clay before adsorption (a), after adsorption of IBP (b) and after adsorption of CTC (c).

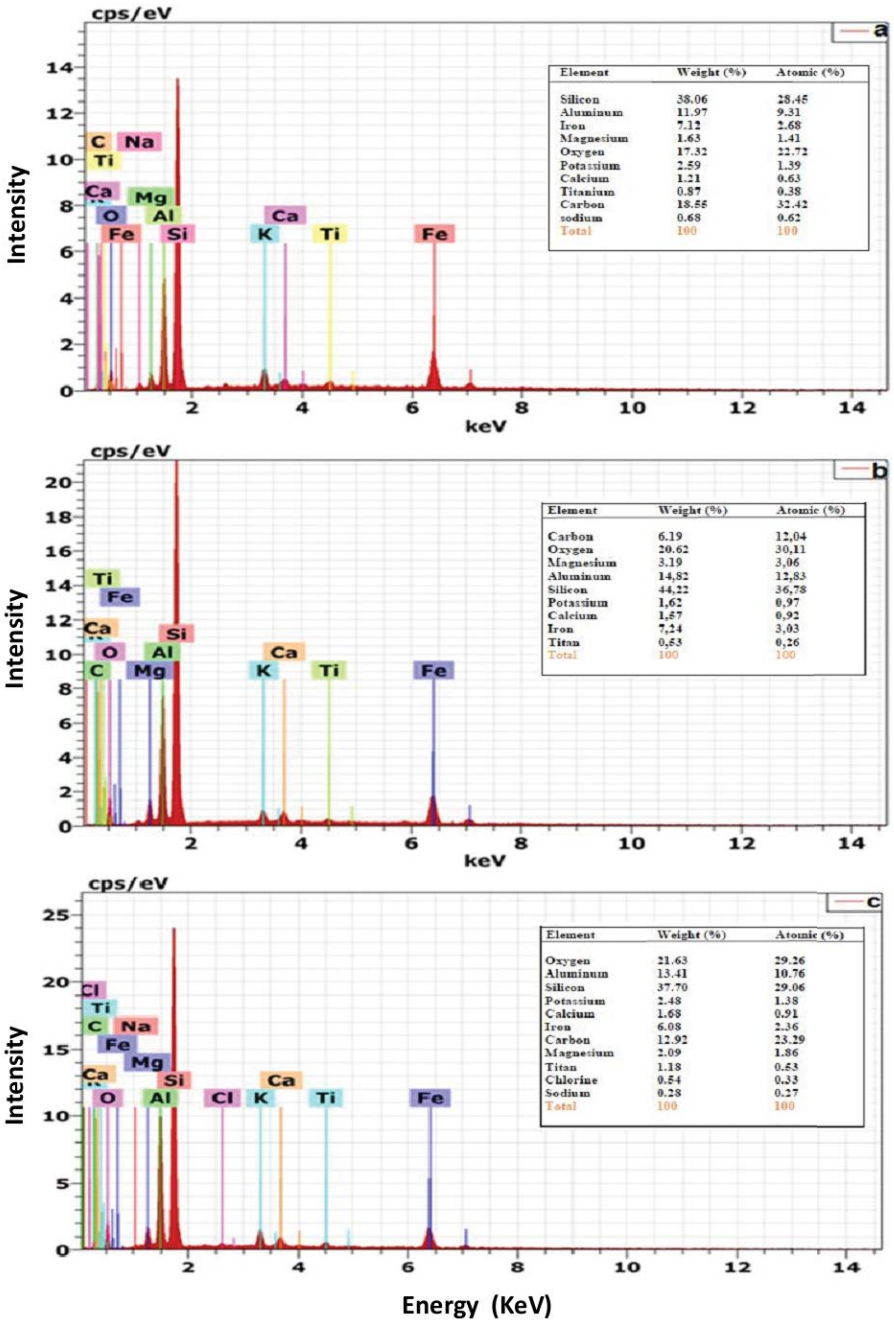


Fig. 10. EDX spectrum of natural clay before adsorption (a), after adsorption of IBP (b) and after adsorption of CTC (c).

iron (Fe), titanium (Ti) and sodium (Na) (Fig. 10a). The EDX peaks of the clay after adsorption (Fig. 10b and c) indicate the disappearance of sodium (Na) in the case of IBP, and the appearance of a new peak, that corresponds to chlorine (Cl) for CTC. These changes prove the retention of both pollutants by our adsorbent. According to these results and the chemical structure and composition of each pollutant, it was deduced that the adsorption of IBP molecules could be explained by cation exchange process [28] and the retention of CTC by clay could be due to electrostatic interactions and the formation of complexes between metal ions and CTC [24].

4. Conclusion

The removal of two drugs (IBP and CTC) from aqueous solutions was carried out by adsorption on natural clay. The sorption of each pollutant was studied at several parameters. The optimal value of the clay concentration is 2 g/L with an initial concentration of 50 mg/L of both xenobiotic. A fast kinetic was found for the antibiotic CTC, and the adsorbed quantity at equilibrium was 24.515 mg/g with an adsorption efficiency of 98.50% at 90 min and pH = 7. Furthermore, the adsorbed quantity of IBP at equilibrium was 14.00 mg/g with an efficiency of

Table 5
Comparison of the maximum adsorbed quantity of IBP and CTC on different adsorbents

Molecules	Adsorbent	Q_m (mg/g)	Reference
IBP	Activated carbon	417	[11]
	Activated carbon	105.91	[17]
	Raw clay	47.84	This work
	Kaolinite	3.1	[31]
	Montmorillonite	6.1	[31]
	Clay micelle complex	62.5	[34]
	Raw clay	3.52	[50]
CTC	Iron(III)-loaded cellulose nanofibers	232.56	[19]
	Illite/Smectite clay	159.7	[33]
	Raw clay	177.7	[44]
	Raw clay	67.567	This work
	Sugarcane bagasse biochar (SBB)	25.740	[51]
	Corn cob biochar (CCB)	36.118	[51]
	Standard activated carbon (SAC)	377.537	[52]
	NH_4Cl-modified activated carbon	482.466	[52]

56.02% at 120 min and pH = 4. The pseudo-second-order model fits well the sorption kinetics of both pollutants. In addition, Langmuir's model gives the highest correlation coefficients for the adsorption of the two micro pollutants. The thermodynamic study of the adsorption of IBP and CTC on raw clay indicates that the adsorption process of CTC was spontaneous and non-spontaneous for IBP. Moreover, the adsorption of both drugs is exothermic and the distribution of the molecules after adsorption increases. The characterization of the clay before and after adsorption confirms the adsorption of CTC and IBP on raw clay. It was found that this clay was very efficient without any further modification as a natural adsorbent for both drugs, especially for the CTC. Table 5 summarise the results of recent works realized on different adsorbents. The studied clay shows remarkable results compared to other adsorbents (Table 5). This abundant clay could be considered as a promising less expensive and environmentally friendly adsorbent for the removal of other pharmaceuticals from aqueous systems.

Symbols

A	—	Initial sorption rate, mg/g min
B	—	Extent of surface coverage, g/mg
A_T	—	Temkin constant, mg/g
B_T	—	Temkin constant, kJ/mol
C_a	—	Adsorbent concentration, g/L
C_e	—	Equilibrium adsorption concentration, mg/L
C_i	—	Initial concentration, mg/L
C_t	—	Concentration of pollutant at time t, mg/L
E	—	Adsorption efficiency, %
K_1	—	Rate constant of the pseudo-first-order, min^{-1}
K_2	—	Rate constant of the pseudo-second-order, g/mg min
K_f	—	Freundlich adsorption constant, L/mg
K_L	—	Langmuir adsorption constant, L/mg
K_d	—	Distribution coefficient
m	—	Mass, g
pH_{PZC}	—	pH of zero charge
pKa	—	Acidity constant
Q_e	—	Equilibrium adsorption capacity, mg/g
Q_{exp}	—	Experimental adsorption capacity, mg/g
Q_{cal}	—	Calculated adsorption capacity, mg/g
Q_m	—	Maximum adsorption capacity, mg/g
Q_t	—	Adsorption capacity at time t, mg/g
R	—	Gas constant, 8.31 J/mol K
R_L	—	Equilibrium parameter of Langmuir
ΔH	—	Enthalpy, kJ/mol
ΔG	—	Gibbs free energy, kJ/mol
ΔS	—	Entropy, J/mol K

References

[1] R. Khatun, Water pollution: causes, consequences, prevention method and role of WBPHED with special reference from Murshidabad District, Int. J. Sci. Res. Publ., 7 (2017) 269–277.
[2] X.L. Qu, P.J.J. Alvarez, Q.L. Li, Applications of nanotechnology in water and wastewater treatment, Water Res., 47 (2013) 3931–3946.
[3] D. Balarak, M. Baniasadi, S.-M. Lee, M.J. Shim, Ciprofloxacin adsorption onto *Azolla filiculoides* activated carbon from aqueous solutions, Desal. Water Treat., 218 (2021) 444–453.
[4] D. Morales-Serrato, J. Torres-Pérez, D.J. de Jesús Ruíz-Baltazar, S.Y. Reyes-López, Adsorbent materials for emerging contaminant (tetracycline) removal, Int. J. Res. GRANTHAALAYAH, 9 (2021) 446–491.
[5] G.Z. Kyzas, J. Fu, N.K. Lazaridis, D.N. Bikiaris, K.A. Matis, New approaches on the removal of pharmaceuticals from wastewaters with adsorbent materials, J. Mol. Liq., 209 (2015) 87–93.
[6] C.G. Daughton, T.A. Ternes, Pharmaceuticals and personal care products in the environment: agents of subtle change?, Environ. Health Perspect., 107 (1999) 907–938.
[7] O. Benhabiles, N. Chekir, D. Tassalit. S. Mahidine, N. Kasbadji Merzouk, Dégradation Solaire d'un polluant pharmaceutique sur un support photocatalytique, Int. J. Sci. Res. Eng. Technol., 3 (2015) 107–113.

[8] T.M. Defarges, M. Guerbet, J. Massol, Impact des médicaments sur l'environnement : état des lieux, évaluation des risques, communication, Therapie, 66 (2011) 335–340.
[9] C. Gadipelly, A. Pérez-González, G.D. Yadav, I. Ortiz, R. Ibáñez, V.K. Rathod, K.V. Marathe, Pharmaceutical industry wastewater: review of the technologies for water treatment and reuse, Ind. Eng. Chem. Res., 53 (2014) 11571–11592.
[10] A.M. Deegan, B. Shaik, K. Nolan, K. Urell, M. Oelgemöller, J. Tobin, A. Morrissey, Treatment options for wastewater effluents from pharmaceutical companies, Int. J. Environ. Sci. Technol., 8 (2011) 649–666.
[11] M.J. Ahmed, Adsorption of non-steroidal anti-inflammatory drugs from aqueous solution using activated carbons: review, J. Environ. Manage., 190 (2017) 274–282.
[12] J. Manrique, F. Martínez, Solubility of ibuprofen in some ethanol + water cosolvent mixtures at several temperatures, Lat. Am. J. Pharm., 26 (2007) 344–354.
[13] A.S. Mestre, J. Pires, J.M.F. Nogueira, A.P. Carvalho, Activated carbons for the adsorption of ibuprofen, Carbon, 45 (2007) 1979–1988.
[14] V. González-Naranjo, K. Boltes, M. Biel, Mobility of ibuprofen, a persistent active drug, in soils irrigated with reclaimed water, Plant Soil Environ., 59 (2013) 68–73.
[15] J.R. Lawrence, G.D.W. Swerhone, L.I. Wassenaar, T.R. Neu, Effects of Selected pharmaceuticals on riverine biofilm communities, Can. J. Microbiol., 51 (2005) 655–669.
[16] A. Ghauch, A.M. Tuqan, N. Kibbi, Ibuprofen removal by heated persulfate in aqueous solution: a kinetics study, Chem. Eng. Sci., 197 (2012) 483–492.
[17] A.F.M. Streit, G.C. Collazzo, S.P. Druzian, R.S. Verdi, E.L. Foletto, L.F.S. Oliveira, G.L. Dotto, Adsorption of ibuprofen, ketoprofen and paracetamol onto activated carbon prepared from effluent treatment plant sludge of the beverage industry, Chemosphere, 262 (2021) 128322, doi: 10.1016/j.chemosphere.2020.128322.
[18] G. Abu-Rumman, T.J. Al-Musawi, M. Sillanpää, D. Balarak, Adsorption performance of an amine-functionalized MCM–41 mesoporous silica nanoparticle system for ciprofloxacin removal in a batch system, Environ. Nanotechnol. Monit. Manage., 16 (2021) 100536, doi: 10.1016/j.enmm.2021.100536.
[19] L. Lu, M. Liu, Y. Chen, Y. Luo, Effective removal of tetracycline antibiotics from wastewater using partially applicable iron(III)-loaded cellulose nanofibers, R. Soc. Open Sci., 8 (2021) 210336, doi: 10.1098/rsos.210336.
[20] K.S.D. Premarathna, A.U. Rajapaksha, N. Adassoriya, B. Sarkar, N.M.S. Sirimuthu, A. Cooray, Y.S. Ok, M. Vithanage, Clay-biochar composites for sorptive removal of tetracycline antibiotic in aqueous media, J. Environ. Manage., 238 (2019) 315–322.
[21] D. Liu, P. Chen, X. Yang, J. Wang, Synthesis and evaluation of bisulfate/mesylate-conjugated chlortetracycline with high solubility and bioavailability, Acta Pharm., 70 (2020) 483–498.
[22] L. Han, H. Zhang, Z. Long, Q. Ge, J. Mei, Y. Yu, H. Fang, Exploring microbial community structure and biological function in manured soil during ten repeated treatments with chlortetracycline and ciprofloxacin, Chemosphere, 228 (2019) 469–477.
[23] K.L. Nelson, V.S. Brözel, S.A. Gibson, R. Thaler, S.A. Clay, Influence of manure from pigs fed chlortetracycline as growth promotant on soil microbial community structure, World J. Microbiol. Biotechnol., 27 (2011) 659–668.
[24] R. Puicharla, D.P. Mohapatra, S.K. Brar, P. Drogui, S. Auger, R.Y. Surampalli, A persistent antibiotic partitioning and co-relation with metals in wastewater treatment plant—chlortetracycline, J. Environ. Chem. Eng., 2 (2014) 1596–1603.
[25] A. Molaei, A. Lakzian, R. Datta, G. Haghnia, A. Astaraei, M.H. Rasouli-Sadaghiani, M.T. Ceccherini, Impact of chlortetracycline and sulfapyridine antibiotics on soil enzyme activities, Int. Agrophys., 31 (2017) 499–505.
[26] H.A. Younes, R. Khaled, H.M. Mahmoud, H.F. Nassar, M.M. Abdelrahman, F.I. Abo El-Ela, M. Taha, Computational and experimental studies on the efficient removal of diclofenac from water using ZnFe-layered double hydroxide as an environmentally benign absorbent, J. Taiwan Inst. Chem. Eng., 102 (2019) 297–311.
[27] K. Styszko, K. Nosek, M. Motak, K. Bester, Preliminary selection of clay minerals for the removal of pharmaceuticals, bisphenol A and triclosan in acidic and neutral aqueous solutions, C.R. Chim., 18 (2015) 1134–1142.
[28] S. Gu, X. Kang, L. Wang, E. Lichtfouse, C. Wang, Clay mineral adsorbents for heavy metal removal from wastewater: a review, Environ. Chem. Lett., 17 (2019) 629–654.
[29] Z. Dali-Youcef, H. Bouabdasselem, N. Bettahar, Élimination des composés organiques par des argiles locales, C.R. Chim., 9 (2006) 1295–1300.
[30] H. Guedidi, I. Lakehal, L. Reinert, J.-M. Lévêque, N. Bellakhal, L. Duclaux, Removal of ionic liquids and ibuprofen by adsorption on a microporous activated carbon: kinetics, isotherms, and pore sites, Arabian J. Chem., 13 (2020) 258–270.
[31] S.K. Behera, S.Y. Oh, H.S. Park, Sorptive removal of ibuprofen from water using selected soil minerals and activated carbon, Int. J. Environ. Sci. Technol., 9 (2012) 85–94.
[32] V.O. Shikuku, R. Zanella, C.O. Kowenje, F.F. Donato, N.M.G. Bandeira, O.D. Prestes, Single and binary adsorption of sulfonamide antibiotics onto iron-modified clay: linear and nonlinear isotherms, kinetics, thermodynamics, and mechanistic studies, Appl. Water Sci., 8 (2018) 175, doi: 10.1007/s13201-018-0825-4.
[33] W. Wang, G. Tian, L. Zong, Y. Zhou, Y. Knag, Q. Wang, A. Wang, From illite/smectite clay to mesoporous silicate adsorbent for efficient removal of chlortetracycline from water, J. Environ. Sci., 51 (2017) 31–43.
[34] S. Khalaf, F. Al-Rimawi, M. Khamis, S. Nir, L. Scrano, S.A. Bufo, R. Karaman, Efficiency of membrane technology activated charcoal and a clay micelle complex for the removal of ibuprofen and mefenamic acid, Int. J. Case Stud., 4 (2015) 38–78.
[35] S. Lagergren, About the theory of so-called adsorption of soluble substances, Kungliga Svenska Vetenskapsakademiens, Handlingar, 24 (1898) 1–39.
[36] Y.S. Ho, G. McKay, Pseudo-second-order model for sorption process, Process Biochem., 34 (1999) 451–465.
[37] R. Yous, H. Cherifi, R. Khalladi, Kinetic models of competitive adsorption of cadmium–iron mixture on montmorillonite, Desal. Water Treat., 221 (2021) 207–217.
[38] I. Langmuir, The constitution and fundamental properties of solids and liquids. Part I. Solids, J. Am. Chem. Soc., 38 (1916) 2221–2295.
[39] H.M.F. Freundlich, Over the adsorption in solution, J. Phys. Chem., 57 (1906) 385–471.
[40] M.I. Temkin, Adsorption equilibrium and the kinetics of processes on nonhomogeneous surfaces and in the interaction between adsorbed molecules, Zh. Fiz. Khim., 15 (1941) 296–332.
[41] B.S. Metwally, A.A. El-Sayed, E.K. Radwan, A.S. Hamouda, M.N. El-Sheikh, M. Salama, Fabrication, characterization, and dye adsorption capability of recycled modified polyamide nanofibers, Egypt. J. Chem., 61 (2018) 867–882.
[42] M.M. El Bendary, E.K. Radwan, M.F. El-Shahat, Valorization of secondary resources into silica-based adsorbents: preparation, characterization and application in dye removal from wastewater, Environ. Nanotechnol. Monit. Manage., 15 (2021) 100455, doi: 10.1016/j.enmm.2021.100455.
[43] S. Patel, S. Mondal, S.K. Majumder, P. Das, P. Ghosh, Treatment of a pharmaceutical industrial effluent by a hybrid process of advanced oxidation and adsorption, ASC Omega, 5 (2020) 32305–32317.
[44] G. Lü, L. Wu, X. Wang, L. Liao, X. Wang, Adsorption of chlortetracycline from water by rectories, Chin. J. Chem. Eng., 20 (2012) 1003–1007.
[45] T. El Malah, H.F. Nour, E.K. Radwan, R.E. Abdel Mageid, T.A. Khattab, M.A. Olson, A bipyridinium-based polyhydrazone adsorbent that exhibits ultrahigh adsorption capacity for the anionic azo dye, direct blue 71, Chem. Eng. J., 409 (2021) 128195, doi: 10.1016/j.cej.2020.128195.
[46] D. Balarak, A.H. Mahvi, S. Shahbaksh, M.A. Wahab, A. Abdala, Adsorptive removal of azithromycin antibiotic from aqueous

solution by *Azolla filiculoides*-based activated porous carbon, Nanomaterials, 11 (2021) 3281, doi: 10.3390/nano11123281.
[47] T. Thiebault, M. Boussafir, L. Le Forestier, C. Le Milbeau, L. Monnin, R. Guégan, Competitive adsorption of a pool of pharmaceuticals onto a raw clay mineral, RSC Adv., 6 (2016) 65257–65265.
[48] A.S. Zdravković, N. Stanković, N.N. Ristić, G.M. Petković, Application of activated bentonite for the removal of direct and reactive dye from aqueous solutions, Chem. Ind. Chem. Eng. Q., 25 (2019) 341–351.
[49] E.K. Radwan, M.E. El-Naggar, A. Abdel-Karim, A.R. Wassel, Multifunctional 3D cationic starch/nanofibrillated cellulose/silver nanoparticles nanocomposite cryogel: synthesis, adsorption, and antibacterial characteristics, Int. J. Biol. Macromol., 189 (2021) 420–431.
[50] H. Khazri, I. Ghorbel-Abid, R. Kalfat, M. Trabelsi-Ayadi, Removal of ibuprofen, naproxen and carbamazepine in aqueous solution onto natural clay: equilibrium, kinetics, and thermodynamic study, Appl. Water Sci., 7 (2017) 3031–3040.
[51] L. Zhang, L. Tong, P. Zhu, P. Huang, Z. Tan, F. Qin, W. Shi, M. Wang, H. Nie, G. Yan, H. Huang, Adsorption of chlortetracycline onto biochar derived from corn cob and sugarcane bagasse, Water Sci. Technol., 78 (2018) 1336–1347.
[52] A. Alahabadi, A. Hosseini-Bandegharaei, G. Moussavi, B. Amin, A. Rastegar, H. Karimi-Sani, M. Fattahi, M. Miri, Comparing adsorption properties of NH_4Cl-modified activated carbon towards chlortetracycline antibiotic with those of commercial activated carbon, J. Mol. Liq., 232 (2017) 367–381.

Supplementary information

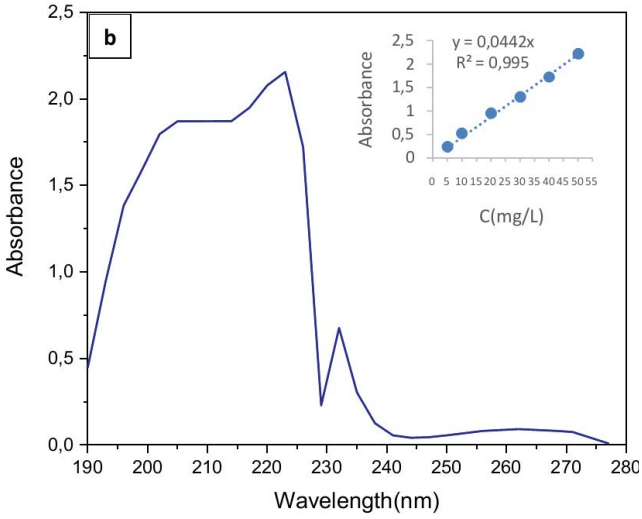


Fig. S1. UV-visible spectra of IBP at C = 50 mg/L and calibration curve at 222 nm.

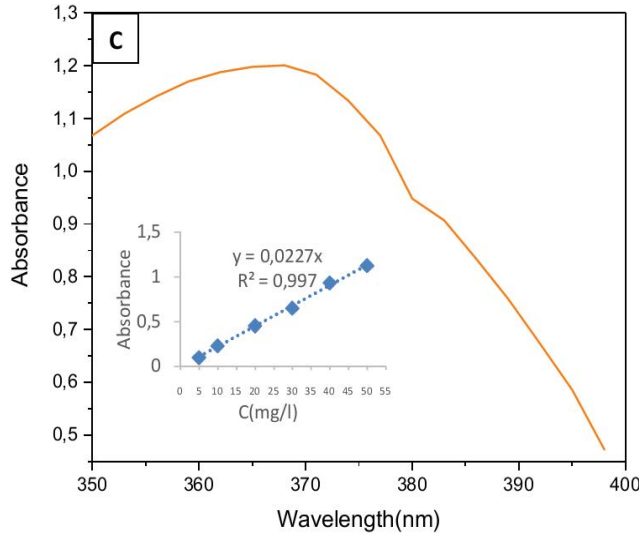


Fig. S2. UV-visible spectra of CTC at C = 50 mg/L and calibration curve of at 370 nm.

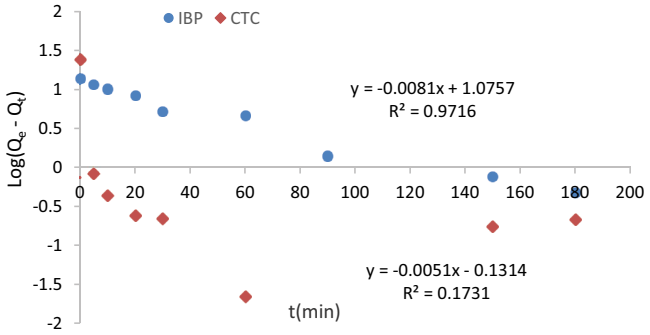


Fig. S3. Pseudo-first-order kinetic adsorption of IBP and CTC onto raw clay (m = 0.1 g/50 mL; C_0 = 50 mg/L; pH_{IBP} = 4; pH_{CTC} = 7).

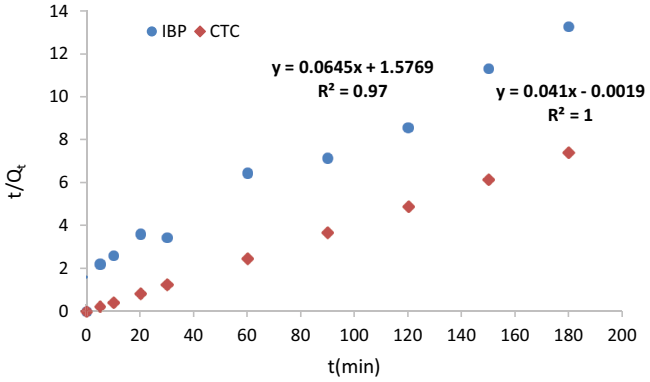


Fig. S4. Pseudo-second-order kinetic adsorption of IBP and CTC onto raw clay (m = 0.1 g/50 mL; C_0 = 50 mg/L; pH_{IBP} = 4; pH_{CTC} = 7).

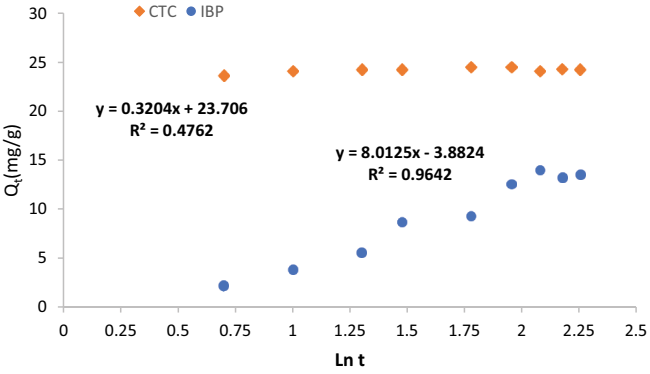


Fig. S5. Elovich model kinetic adsorption of IBP and CTC onto raw clay (m = 0.1 g/50 mL; C_0 = 50 mg/L; pH_{IBP} = 4; pH_{CTC} = 7).

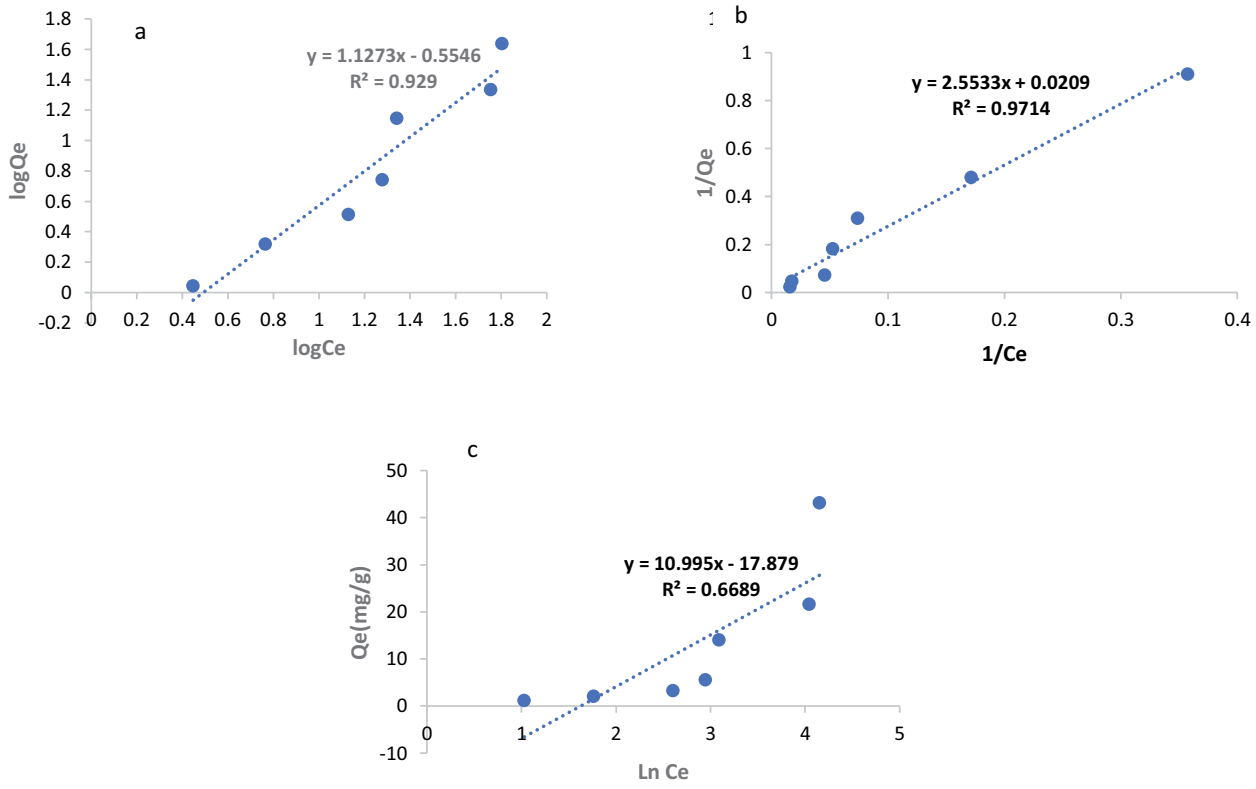


Fig. S6. Models fitting of adsorption isotherms of IBP: (a) Freundlich, (b) Langmuir, and (c) Temkin.

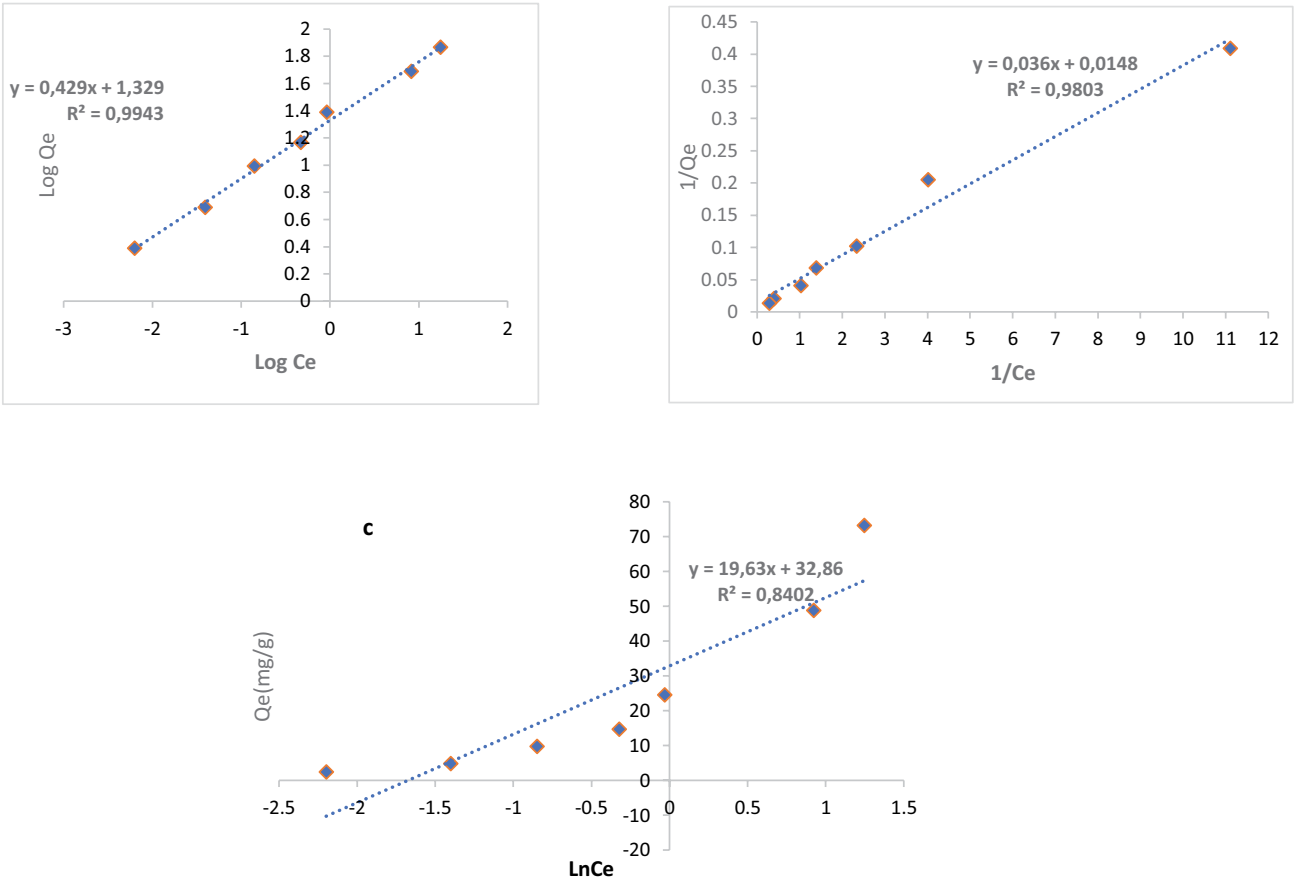


Fig. S7. Models fitting of adsorption isotherms of CTC: (a) Freundlich, (b) Langmuir, and (c) Temkin.